

DSCC2015-9900

ROBUST ATTITUDE TRACKING CONTROL FOR A QUADROTOR BASED ON THE UNCERTAINTY AND DISTURBANCE ESTIMATOR

Jiguo Dai, Qi Lu, Beibei Ren*

Department of Mechanical Engineering
Texas Tech University
Lubbock, Texas, 79409

Email: jiguo.dai@ttu.edu, qi.lu@ttu.edu, beibei.ren@ttu.edu

Qing-Chang Zhong

Department of Electrical and Computer Engineering
Illinois Institute of Technology
Chicago, Illinois 60616
Email: zhongqc@iit.edu

ABSTRACT

In this paper, a robust control method based on the uncertainty and disturbance estimator (UDE) is developed to achieve the attitude tracking control for a quadrotor. To facilitate the control design, the coupled terms in the roll, pitch and yaw dynamics are lumped into the uncertainty term and the remained dynamics can be regarded as decoupled subsystems. As a result, for each subsystem, the lumped uncertainty term contains all the coupled terms, uncertainties and disturbances, then the UDE method is applied for the uncertainty compensation. Compared with the existing UDE control works, the introduced filtered tracking error dynamics simplifies the controller design and implementation. Furthermore, the stability analysis of the closed-loop system is established and experimental studies are carried out to illustrate the effectiveness of the developed control method.

INTRODUCTION

As a promising autonomous system, the quadrotor is designed to fly in complex environments to complete specific missions while offering great autonomy, like rescue and search, remote inspection, surveillance, military applications [1]. The quadrotor has advantages of small size, light weight and ability of vertically taking off and landing. Thus, it holds high maneuverability and has attracted much attention from the research communities.

In order to achieve the desired performance, there are usually two sub-problems in the control for the quadrotor : (a) the at-

titude control; (b) the position control [2]. The dynamics analysis shows that the position and attitude subsystems of the quadrotor are cascade interconnected [2, 3]. Since the position controller generates a reference attitude set points for the attitude controller, the control problem mainly focuses on the attitude control [4–6]. Furthermore, the complex working environment, various payloads, lacking of accurate model knowledge will generate internal uncertainties and external disturbances. The uncertainties and disturbances compensation is an challenging problem in engineering applications. In this paper, the quadrotor attitude control problem in the presence of coupled dynamics, modeling uncertainties and external disturbances is considered.

The quadrotor attitude control has been investigated using various control methods [4, 7–12]. The effectiveness of classical PID (proportional-integral-derivative) controller and LQ (linear quadratic) were investigated in [4]. However, these linear controllers are not easy to deal with the highly nonlinearities. Since the model-based controllers, such as feedback linearization [13], dynamic inversion [7], require the exact knowledge of the model, they cannot handle the uncertainties. The sliding mode control is robust to the large uncertainties, but its switching logic will lead to the chattering phenomenon [8, 9]. The robust methods in frequency domain like H_2 , H_∞ control methods introduced in [11, 12] work well only within a frequency bandwidth limit.

In this paper, in order to achieve the attitude control of the quadrotor in the presence of internal uncertainties and external disturbances, a control method based on the uncertainty and disturbance estimator (UDE) is adopted. The UDE method, which was proposed in [14], has many advantages in both design and

*Address all correspondence to this author.

implementation respects and its excellent performance in handling the uncertainty and disturbance yet with very easy tuning and implementation has been demonstrated in recent years through both theories (including extensions to both linear [14,15] and nonlinear systems [16–20], systems with delays [15,17] etc.) and wide applications (covering mechatronics and robotics [21], electrical machines and drives [14, 20], renewable energy [22], aerospace and automotive systems [23,24] etc). The basic idea of the UDE method is that in the frequency domain an engineering signal (the lumped system uncertainty and external disturbance) can be approximated by putting it through a filter with the appropriate bandwidth. The main contributions of this paper are as follows:

1) Extending the UDE method to the decoupling control. The key idea is that lumping the coupled dynamics into an uncertainty term, such that the remained dynamics can be regarded as decoupled subsystems. For each subsystem, the UDE method can be applied individually for the uncertainties compensation.

2) Compared with the existing UDE control works, the filtered tracking error dynamics is introduced to simplify the controller design and implementation.

The rest of this paper is organized as follows. Section 2 illustrates the preliminaries about the quadrotor dynamics. Section 3 is devoted to system decoupling and Section 4 presents the attitude tracking controller design. The stability analysis of the closed-loop system is presented in Section 5 and the experiment results are shown in Section 6. Finally, Section 7 gives the conclusions.

PROBLEM FORMULATION AND PRELIMINARY

As shown in Fig.1, the quadrotor has six degree of freedoms which are controlled by four rotors installed in its arms. The rotation of these propellers generates upward lifting forces and torques along their spinning axes. Two of these propellers rotate clockwise and the remaining rotate anticlockwise. The quadrotor adjusts its height, position, yaw, pitch, roll and completes taking-off, landing actions by changing the speeds of four rotors. The dynamic model is under those assumptions: the structure of quadrotor is supposed to be rigid and symmetric, thrust and drag are supposed to be proportional to the square of rotor speed and the origin of the body frame is fixed at the center of mass.

The thrust and torque generated by each propeller is defined by

$$f_k = b\omega_k^2 \quad (1)$$

$$\tau_k = d\omega_k^2, \quad k = 1, 2, 3, 4 \quad (2)$$

where ω_k is the angular speed of k th motor, b is the positive thrust constant, and d is the positive drag constant. The torques

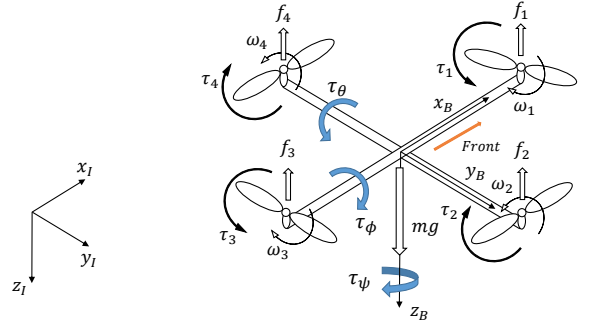


Figure 1. Quadrotor configuration

generated by the motors along the three body axes, x_B , y_B and z_B , can be expressed as

$$\tau_\phi = l(f_4 - f_2) = bl(\omega_4^2 - \omega_2^2) \quad (3)$$

$$\tau_\theta = l(f_3 - f_1) = bl(\omega_3^2 - \omega_1^2) \quad (4)$$

$$\begin{aligned} \tau_\psi &= \tau_2 + \tau_4 - \tau_1 - \tau_3 \\ &= d(\omega_2^2 + \omega_4^2 - \omega_1^2 - \omega_3^2) \end{aligned} \quad (5)$$

where l is the distance from the motors to the center of mass. Consequently, the attitude dynamics is modeled as follows [4]

$$\ddot{\phi} = \dot{\theta}\psi \left(\frac{I_{yy} - I_{zz}}{I_{xx}} \right) - \frac{J}{I_{xx}} \dot{\theta}\Omega + \frac{1}{I_{xx}} \tau_\phi \quad (6)$$

$$\ddot{\theta} = \dot{\phi}\psi \left(\frac{I_{zz} - I_{xx}}{I_{yy}} \right) + \frac{J}{I_{yy}} \dot{\phi}\Omega + \frac{1}{I_{yy}} \tau_\theta \quad (7)$$

$$\ddot{\psi} = \dot{\theta}\dot{\phi} \left(\frac{I_{xx} - I_{yy}}{I_{zz}} \right) + \frac{1}{I_{zz}} \tau_\psi \quad (8)$$

where ϕ, θ, ψ are the roll, pitch and yaw angles and I_{xx}, I_{yy}, I_{zz} are the moments of inertia. J denotes the inertia of propeller and $\Omega = \omega_2 + \omega_4 - \omega_1 - \omega_3$. The generalized coordinates are chosen as $p(t) = [\phi, \theta, \psi]^T$, $q(t) = [\dot{\phi}, \dot{\theta}, \dot{\psi}]^T$, and the control input is $u(t) = [\tau_\phi, \tau_\theta, \tau_\psi]^T$. Assume that the system has an external acceleration disturbance $d(t)$ which might be caused by modeling errors, wind or other environmental factors, then equations (6)-(8) can be written in the following forms

$$\dot{p}(t) = q(t) \quad (9)$$

$$\dot{q}(t) = f(p, q) + g(p, q)u(t) + d(t) \quad (10)$$

$$\text{with } f(p, q) = \begin{bmatrix} \dot{\theta}\psi \left(\frac{I_{yy} - I_{zz}}{I_{xx}} \right) - \frac{J}{I_{xx}} \dot{\theta}\Omega \\ \dot{\phi}\psi \left(\frac{I_{zz} - I_{xx}}{I_{yy}} \right) + \frac{J}{I_{yy}} \dot{\phi}\Omega \\ \dot{\theta}\dot{\phi} \left(\frac{I_{xx} - I_{yy}}{I_{zz}} \right) \end{bmatrix}, \quad g(p, q) = \begin{bmatrix} \frac{1}{I_{xx}} & 0 & 0 \\ 0 & \frac{1}{I_{yy}} & 0 \\ 0 & 0 & \frac{1}{I_{zz}} \end{bmatrix},$$

which is non-singular.

A set of continuous smooth and bounded reference signals are given as

$$r_d(t) = [\phi_d, \theta_d, \psi_d]^T \in C^2(\mathbb{R}^3) \cap L^2(\mathbb{R}^3) \quad (11)$$

where $C^2(\cdot)$ and $L^2(\cdot)$ are the function spaces of second differential and bounded functions.

The objective is to design a robust control algorithm for the quadrotor system (9) and (10) to force the states $p(t) = [\phi, \theta, \psi]^T$ to asymptotically track the reference signals $r_d(t)$ in (11), i.e., to achieve

$$p(t) \rightarrow r_d \text{ as } t \rightarrow \infty. \quad (12)$$

SYSTEM DECOUPLING

In the system dynamics (10),

$$f(p, q) = f_c(t) + \Delta f(t) \quad (13)$$

where $f_c(t) = \begin{bmatrix} \dot{\theta}\psi \left(\frac{I_{yy}-I_{zz}}{I_{xx}} \right) \\ \dot{\phi}\psi \left(\frac{I_{zz}-I_{xx}}{I_{yy}} \right) \\ \dot{\theta}\phi \left(\frac{I_{xx}-I_{yy}}{I_{zz}} \right) \end{bmatrix}$ denote the coupled terms and $\Delta f(t) = \begin{bmatrix} -\frac{J}{I_{xx}}\dot{\theta}\Omega \\ \frac{J}{I_{yy}}\dot{\phi}\Omega \\ 0 \end{bmatrix}$ denote the uncertainty terms since the parameter J is unknown.

Then the system dynamics (9), (10) can be written as

$$\dot{p}(t) = q(t) \quad (14)$$

$$\begin{aligned} \dot{q}(t) &= (f_c(t) + \Delta f(t) + d(t)) + g(p, q)u(t) \\ &= u_d(t) + g(p, q)u(t) \end{aligned} \quad (15)$$

where $u_d(t) = f_c(t) + \Delta f(t) + d(t)$ includes all the coupled states, uncertainties and disturbances.

Since $g(p, q)$ is diagonal and invertible and $u_d(t)$ is regarded as the lumped uncertainty term, the system (14), (15) can be decoupled into a set of second order ODEs. For each subsystem, the system dynamics becomes

$$\begin{aligned} \dot{p}_i(t) &= q_i(t) \\ \dot{q}_i(t) &= u_{di}(t) + g_{ii}u_i(t) \end{aligned} \quad (16)$$

where $i = 1, 2, 3$ denote the roll, pitch and yaw, respectively.

CONTROLLER DESIGN

Once the system is decoupled into three second-order subsystems (16), the UDE-based controller for each subsystem will be designed following the procedures in [14].

The tracking error vector for each subsystem is defined as

$$e_i(t) = [r_{di}(t) - p_i(t), \dot{r}_{di}(t) - q_i(t)]^T \quad (17)$$

In order to simplify the controller design and implementation, the filtered tracking error is introduced as follows

$$e_{si}(t) = \lambda_i [r_{di}(t) - p_i(t)] + [\dot{r}_{di}(t) - q_i(t)] \quad (18)$$

where $\lambda_i \in \mathbb{R}$ is chosen such that the polynomial $s + \lambda_i = 0$ has root in the open left half of the complex plane. According to (16), the derivative of the filtered tracking error in (18) with respect to the time t is given by

$$\dot{e}_{si}(t) = \lambda_i [\dot{r}_{di}(t) - q_i(t)] + [\ddot{r}_{di}(t) - u_{di}(t) - g_{ii}u_i(t)] \quad (19)$$

The controller for (19) is chosen as

$$u_i(t) = v_{li}(t) + v_{di}(t) \quad (20)$$

where $v_{li}(t)$ is for the feedback linearization and $v_{di}(t)$ is for the uncertainties compensation. If the term $u_{di}(t)$ in (19) is known, the uncertainties compensation control part can be chosen as

$$v_{di}(t) = -g_{ii}^{-1}u_{di}(t) \quad (21)$$

and the feedback linearization control part $v_{li}(t)$ can be chosen as

$$v_{li}(t) = g_{ii}^{-1}k_{mi}e_{si}(t) + g_{ii}^{-1}\lambda_i[\dot{r}_{di}(t) - q_i] + g_{ii}^{-1}\ddot{r}_{di}(t) \quad (22)$$

where k_{mi} is a positive design parameter and all the signals in (22) are known or measurable. Then substituting (21) and (22) into (20), there is

$$u_i(t) = g_{ii}^{-1}k_{mi}e_{si}(t) + g_{ii}^{-1}\lambda_i[\dot{r}_{di}(t) - q_i] + g_{ii}^{-1}\ddot{r}_{di}(t) - g_{ii}^{-1}u_{di}(t) \quad (23)$$

Furthermore, substituting (23) into (19) results in

$$\dot{e}_{si}(t) = -k_{mi}e_{si}(t) \quad (24)$$

It shows that the closed-loop system is stable and $e_{si}(t)$ will exponentially converge to zero when t tends to infinity. Furthermore, it can be concluded from (17), (18) that the tracking error $e_i(t)$ also exponentially converges to zero when t tends to infinity.

However, $u_{di}(t)$ in (19) is unknown due to uncertainties and disturbances, so the uncertainties compensation control part $v_{di}(t)$ in (21) should be redesigned. Substituting (20), (22) into (19) leads to

$$\dot{e}_{si}(t) = -k_{mi}e_{si}(t) + [-g_{ii}v_{di} - u_{di}(t)] \quad (25)$$

Solving $u_{di}(t)$ gives

$$u_{di}(t) = -\dot{e}_{si}(t) - k_{mi}e_{si}(t) - g_{ii}v_{di}(t) \quad (26)$$

It indicates that the lumped uncertainty term can be observed by the filtered tracking error and the control signal. As shown in [14], adopting a strictly proper low-pass filter $G_{fi}(s)$ with unity gain and zero phase shift in the spectrum of $u_{di}(t)$, the estimation of $u_{di}(t)$ is obtained as

$$\hat{u}_{di}(t) = \mathcal{L}^{-1}\{G_{fi}(s)\} * [-\dot{e}_{si}(t) - k_{mi}e_{si}(t) - g_{ii}v_{di}(t)] \quad (27)$$

where $\hat{u}_{di}(t)$ is the estimation of $u_{di}(t)$ and \mathcal{L}^{-1} is the inverse-Laplace transform operator. Selecting

$$v_{di}(t) = -g_{ii}^{-1}\hat{u}_{di}(t) \quad (28)$$

and using (27) lead to

$$v_{di}(t) = -g_{ii}^{-1}\mathcal{L}^{-1}\{G_{fi}(s)\} * [-\dot{e}_{si}(t) - k_{mi}e_{si}(t) - g_{ii}v_{di}(t)] \quad (29)$$

Solving (29) for $v_{di}(t)$ results in

$$v_{di}(t) = -g_{ii}^{-1}\left(\mathcal{L}^{-1}\left\{\frac{G_{fi}(s)}{1-G_{fi}(s)}\right\} * [-\dot{e}_{si}(t) - k_{mi}e_{si}(t)]\right) \quad (30)$$

Substituting (22) and (30) into (20) leads to the UDE-based controller

$$\begin{aligned} u_i(t) &= g_{ii}^{-1}k_{mi}e_{si}(t) + g_{ii}^{-1}\lambda_i[\dot{r}_{di}(t) - q_i] + g_{ii}^{-1}\ddot{r}_{di}(t) \\ &\quad - g_{ii}^{-1}\left(\mathcal{L}^{-1}\left\{\frac{G_{fi}(s)}{1-G_{fi}(s)}\right\} * [-\dot{e}_{si}(t) - k_{mi}e_{si}(t)]\right) \end{aligned} \quad (31)$$

STABILITY ANALYSIS

The overall control system is depicted in Fig. 2 and the performance is analyzed in the following theorem.

Theorem 1. Consider the closed-loop system consisting of the plant (16), the reference signals (11) and the control law (31). Then for any initial value, the filtered tracking error will remain within the compact set $\Omega_{e_s} := \{e_s \in \mathbb{R} | \|e_s\|^2 \leq \max\{\gamma, e_{si}^2(0)\}\}$, with $\gamma = \frac{\mu^2\|\tilde{u}_{di}(t)\|_{L^\infty}^2}{2\mu k_{mi}-1}$, which can be adjusted by parameters μ , k_{mi} and the uncertainty estimation error $\tilde{u}_{di}(t) = \hat{u}_{di}(t) - u_{di}(t)$.

Proof. Substituting (20), (22), (28) into (19) results in the following closed-loop system error dynamics

$$\dot{e}_{si}(t) = -k_{mi}e_{si}(t) + \tilde{u}_{di}(t) \quad (32)$$

Choose the following Lyapunov function candidate

$$V_i(t) = \frac{1}{2}e_{si}^2(t) \quad (33)$$

Taking the derivative of $V(t)$ with respect to time t and using (32), there is

$$\begin{aligned} \dot{V}_i(t) &= e_{si}(t)\dot{e}_{si}(t) \\ &= e_{si}(t)[-k_{mi}e_{si}(t) + \tilde{u}_{di}(t)] \end{aligned} \quad (34)$$

By using the Young's inequality, we deduce the following results

$$\begin{aligned} \dot{V}_i(t) &\leq -k_{mi}\|e_{si}(t)\|^2 + \|e_{si}(t)\|\|\tilde{u}_{di}(t)\| \\ &\leq -k_{mi}\|e_{si}(t)\|^2 + \left(\frac{\|e_{si}(t)\|^2}{2\mu} + \frac{\mu\|\tilde{u}_{di}(t)\|^2}{2}\right) \\ &= -\left(k_{mi} - \frac{1}{2\mu}\right)\|e_{si}(t)\|^2 + \frac{\mu}{2}\|\tilde{u}_{di}(t)\|^2 \\ &= -\beta_1\|e_{si}(t)\|^2 + \beta_2\|\tilde{u}_{di}(t)\|^2 \end{aligned} \quad (35)$$

where $\mu > 0$, $\beta_2 = \frac{\mu}{2} > 0$ and $\beta_1 = k_{mi} - \frac{1}{2\mu} > 0$.

According to (33), there is

$$\dot{V}_i(t) \leq -2\beta_1 V_i(t) + \beta_2 \|\tilde{u}_{di}(t)\|^2 \quad (36)$$

Let $c_1 = 2\beta_1$ and $c_2 = \beta_2\|\tilde{u}_{di}(t)\|^2$, there is

$$\dot{V}_i(t) \leq -c_1 V_i(t) + c_2 \quad (37)$$

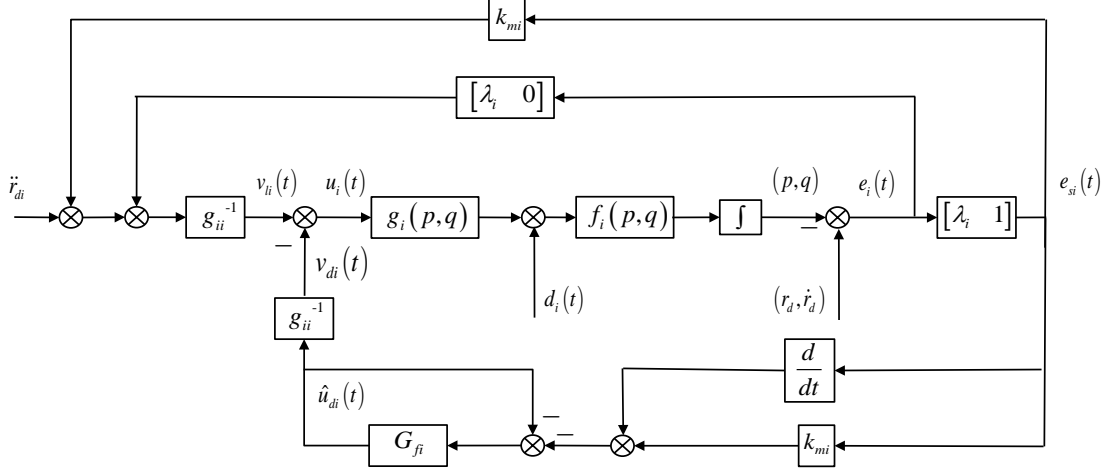


Figure 2. UDE-based control framework

then

$$V_i(t) \leq V_i(0)e^{-c_1 t} + \frac{c_2}{c_1} (1 - e^{-c_1 t}) \quad (38)$$

Noting (33) and $V_i(0) = \frac{1}{2}e_{si}^2(0)$, it can be derived that

$$\|e_{si}(t)\|^2 \leq e_{si}^2(0)e^{-c_1 t} + \frac{2c_2}{c_1} (1 - e^{-c_1 t}) \quad (39)$$

As $c_1 > 0$, the first term on the right hand side of (39) will decay to 0. The second term on the right hand side is bounded by $\frac{2c_2}{c_1}$, which can be further expressed as

$$\begin{aligned} \frac{2c_2}{c_1} &\leq \frac{\mu^2 \|\tilde{u}_{di}(t)\|^2}{2\mu k_{mi} - 1} \\ &\leq \frac{\mu^2 \|\tilde{u}_{di}(t)\|_{L^\infty}^2}{2\mu k_{mi} - 1} \\ &:= \gamma \end{aligned} \quad (40)$$

Therefore, the filtered tracking error remains within the compact set $\Omega_{e_s} := \left\{ e_{si} \in \mathbb{R} \mid \|e_{si}\|^2 \leq \max\{\gamma, e_{si}^2(0)\} \right\}$. The bound radius γ is determined by control parameters μ , k_{mi} and the uncertainty estimation error $\|\tilde{u}_{di}(t)\|$. \square

Corollary 1. Under the same conditions of Theorem 1, the tracking error of the system will be bounded, i.e. $\|e_i(t)\| \leq \max\{\|e_i(0)\|, \sqrt{\gamma}, \|e_{si}(0)\|\}$.

Corollary 2. While under the conditions $\beta_1 = k_{mi} - \frac{1}{2\mu} > 0$ and the estimation of the uncertainty is accurate enough, that



Figure 3. AscTec Hummingbird Quadrotor

is, $\lim_{t \rightarrow \infty} \tilde{u}_{di}(t) = 0$, then the system states will asymptotically track the reference, i.e. $\lim_{t \rightarrow \infty} p_i(t) = r_{di}(t)$.

EXPERIMENTAL VALIDATION

In this section, experiments are carried out to verify the effectiveness of the developed control algorithm. The experimental platform is the Hummingbird from Ascending Technologies GmbH(Asctec), as shown in Fig. 3. According to [14], the choice of a first-order low pass filter in the form of

$$G_{fi}(s) = \frac{1}{\tau_i s + 1} \quad (41)$$

is reasonable, where $\tau_i > 0$ is the time constant and covers the spectrum of the lumped uncertainty term $u_{di}(t)$. Then the con-

troller (31) is simplified as

$$\begin{aligned}
u_i(t) &= g_{ii}^{-1} k_{mi} e_{si}(t) + \frac{g_{ii}^{-1}}{\tau_i} e_{si}(t) + g_{ii}^{-1} \frac{k_{mi}}{\tau_i} \int_0^t e_{si}(\xi) d\xi \\
&\quad + g_{ii}^{-1} \lambda_i [\dot{r}_{di}(t) - q_i] + g_{ii}^{-1} \ddot{r}_{di}(t) \\
&= g_{ii}^{-1} \left[k_{mi} + \frac{1}{\tau_i} \right] e_{si}(t) + g_{ii}^{-1} \frac{k_{mi}}{\tau_i} \int_0^t e_{si}(\xi) d\xi \\
&\quad + g_{ii}^{-1} \lambda_i [\dot{r}_{di}(t) - q_i] + g_{ii}^{-1} \ddot{r}_{di}(t)
\end{aligned} \tag{42}$$

The time constant τ_i , controller parameters λ_i and k_{mi} are chosen differently for each subsystem which are listed in the Table 1. In addition, the thrust constant $b = 6.11 \times 10^{-8} N/rpm^2$, the drug constant $d = 1.5 \times 10^{-9} Nm/rpm^2$ [25].

Table 1. UDE based controller parameters

Dof	λ_i	τ_i	k_{mi}
Roll ϕ	0.5	1	4
Pitch θ	0.5	1	4
Yaw ψ	5	2.5	3.5

For comparison, a PID controller

$$u_i^{pid}(t) = g_{ii}^{-1} \left[K_{Pi} (r_{di} - p_i) + K_{Di} (\dot{r}_{di} - q_i) + K_{Ii} \int (r_{di} - p_i) dt \right] \tag{43}$$

is also implemented with the control parameters shown in the Table 2.

Table 2. PID controller parameters

Dof	K_{Pi}	K_{Di}	K_{Ii}
Roll ϕ	3	5	1
Pitch θ	3	5	1
Yaw ψ	8	5	1

Case 1: Nominal Case

The goal of this case is to achieve the roll and pitch angles stabilization, while the yaw angle tracking. The results using the developed UDE-based controller and the PID controller are illustrated in Fig. 4.

The whole experiment period is about 100 seconds. The quadrotor is set to take off at $t = 10s$ and start landing at $t = 90s$. The references of the roll and pitch are set to zero. The yaw reference signal is chosen as follows,

$$r_{d3} = \begin{cases} 180^\circ & t = 0s \sim 20s \\ 210^\circ & t = 20s \sim 40s \\ 180^\circ & t = 40s \sim 50s \\ 150^\circ & t = 60s \sim 80s \\ 180^\circ & t = 80s \sim 90s \end{cases} \tag{44}$$

From Fig. 4 (a), (c), it can be seen that both the UDE based controller and the PID controller could stabilize the roll and pitch angles in the range of $\pm 5^\circ$, which is a moderate steady state error. For the yaw subsystem, in Fig. 4 (e), it shows that the yaw state successfully tracks the yaw reference and the steady state error of UDE based controller is within the range of $\pm 2^\circ$, the PID controller is within the range of $\pm 5^\circ$. And the control inputs of both controllers are shown in Fig. 4 (b), (d), (f).

Case 2: Disturbance Rejection

The goal of this case is to test the robustness of the UDE-based controller and PID controller. The experiment environment and the controller parameters are same with Case 1. The quadrotor is set to take off at $t = 10s$ and start landing at $t = 60s$. The roll and pitch references are set to zero and there are no disturbance applied. The yaw reference is set as 180° and two spike disturbances $d = 50(t - 20)$ and $d = -50(t - 40)$ are applied at $t = 20s$ and $t = 40s$ respectively which can be seen in Fig. 5 (e).

After applying the disturbances at $20s$ and $40s$, both the UDE-based controller and PID controller could stabilize the yaw subsystem. However, it could be seen that the UDE based controller is more robust and has a better disturbance rejection ability than the PID controller. Furthermore, the figures also show that the pitch and roll control performance by the PID is degraded due to the coupling effects of the yaw, while the developed UDE-based control can handle the uncertainty, disturbance, and coupling simultaneously and effectively. Fig. 5 (b), (d), (f) illustrate the control inputs of both controllers for each subsystem.

From both Case 1 and Case 2, the experiment results show the excellent performance of the developed UDE-based controller in handling the uncertainty and disturbance yet with very easy tuning and implementation advantages over the PID controller.

CONCLUSIONS

In this paper, an UDE-based controller for a quadrotor has been developed to achieve the attitude control in the presence

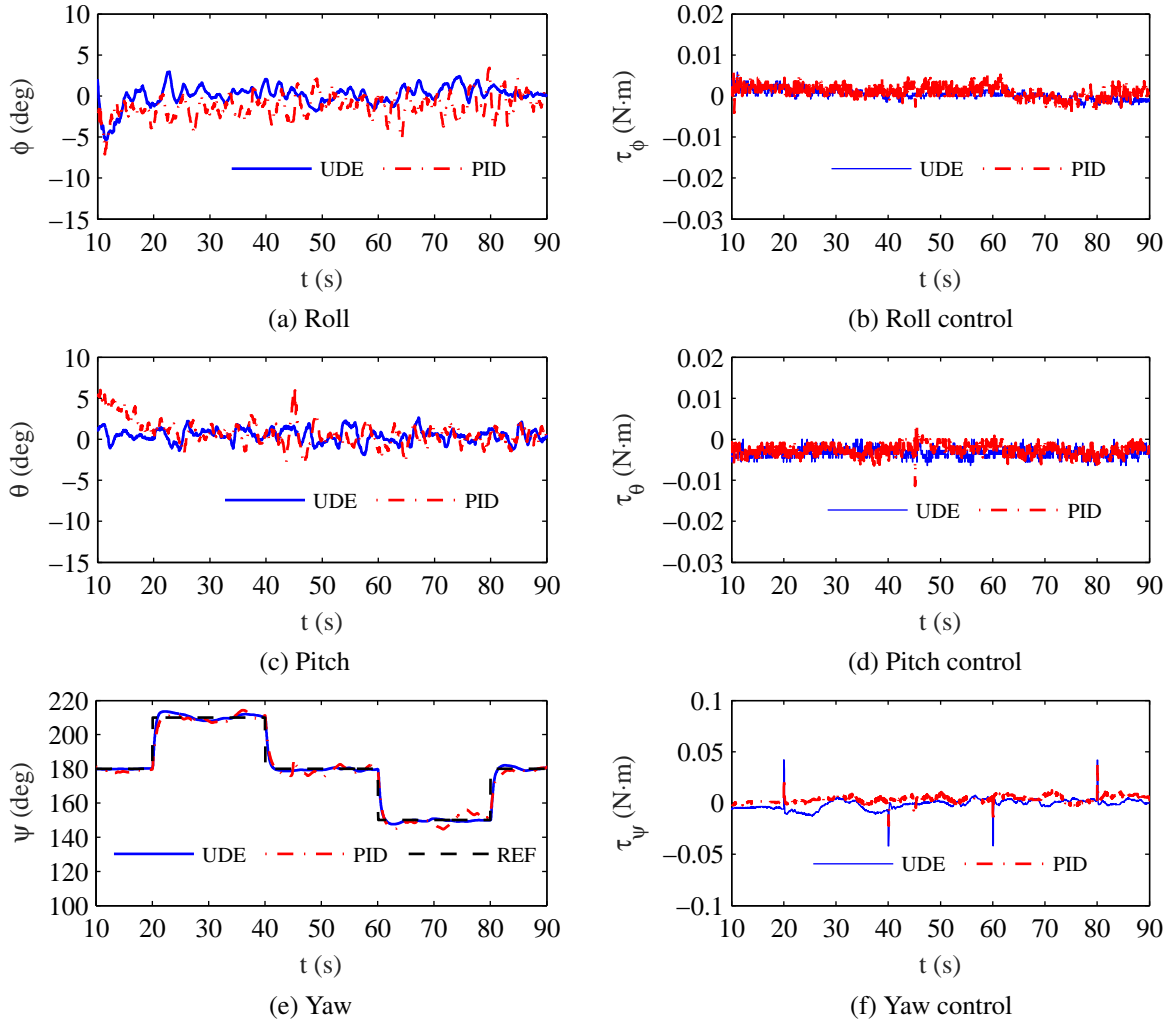


Figure 4. Experimental results for nominal case

of coupled dynamics, internal uncertainties and external disturbances. By regarding the coupled terms in the system as a part of the lumped uncertainty, the nonlinear MIMO system with three degree of freedoms (roll, pitch, yaw) can be decoupled into three decoupled subsystems. Following the UDE-based control design procedure, controllers have been developed for each subsystem to track reference signals. The filtered tracking error dynamics has been introduced to simplify the controller design and implementation. Furthermore, the stability of the closed-loop system has been analyzed and the experiments based on the AscTec Hummingbird platform have verified the effectiveness of the developed method.

ACKNOWLEDGMENT

The authors would like to thank Dr. Pedro Garcia, Universidad Politécnica de Valencia, Spain, for his valuable opinions and

suggestions with the sonar sensor integration.

REFERENCES

- [1] Bouabdallah, S., 2007. “Design and control of quadrotors with application to autonomous flying”. PhD thesis, École Polytechnique federale de Lausanne, Lausanne, Switzerland.
- [2] Fresk, E., and Nikolakopoulos, G., 2013. “Full quaternion based attitude control for a quadrotor”. In Proceedings of the European Control Conference, IEEE, pp. 3864–3869.
- [3] Ryll, M., Bulthoff, H. H., and Robuffo, G. P., 2012. “Modeling and control of a quadrotor UAV with tilting propellers”. In Proceedings of International Conference on Robotics and Automation, IEEE, pp. 4606–4613.
- [4] Bouabdallah, S., Noth, A., and Siegwart, R., 2004. “PID vs

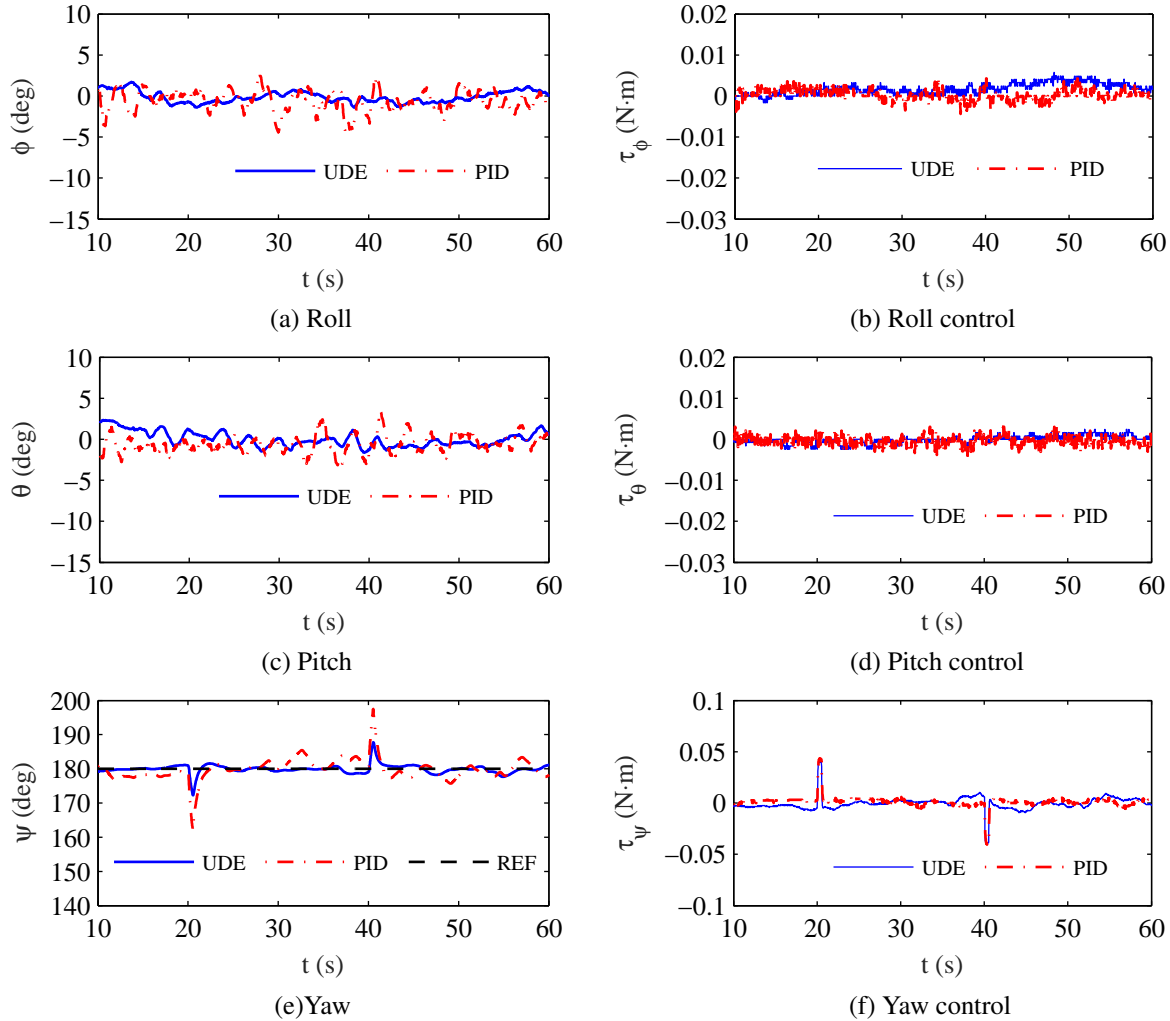


Figure 5. Experimental results for disturbance rejection

- LQ control techniques applied to an indoor micro quadrotor". In Proceedings of the International Conference on Intelligent Robots and Systems, Vol. 3, IEEE, pp. 2451–2456.
- [5] Hoffmann, G. M., Huang, H., Waslander, S. L., and Tomlin, C. J., 2007. "Quadrotor helicopter flight dynamics and control: theory and experiment". In Proceedings of Guidance, Navigation, and Control Conference, Vol. 2, AIAA.
- [6] Islam, S., Liu, P., and El Saddik, A., 2015. "Robust control of four-rotor unmanned aerial vehicle with disturbance uncertainty". *IEEE Transactions on Industrial Electronics*, **62**(3), March, pp. 1563–1571.
- [7] Das, A., Subbarao, K., and Lewis, F., 2009. "Dynamic inversion with zero-dynamics stabilisation for quadrotor control". *IET Control Theory & Applications*, **3**(3), pp. 303–314.
- [8] Besnard, L., Shtessel, Y. B., and Landrum, B., 2012. "Quadrotor vehicle control via sliding mode controller

driven by sliding mode disturbance observer". *Journal of the Franklin Institute*, **349**(2), pp. 658–684.

- [9] Aguilar-Ibáñez, C., Sira-Ramírez, H., Suárez-Castañón, M. S., Martínez-Navarro, E., and Moreno-Armendariz, M. A., 2012. "The trajectory tracking problem for an unmanned four-rotor system: flatness-based approach". *International Journal of Control*, **85**(1), pp. 69–77.
- [10] Lee, T., Leok, M., and McClamroch, N. H., 2013. "Nonlinear robust tracking control of a quadrotor UAV on SE (3)". *Asian Journal of Control*, **15**(2), pp. 391–408.
- [11] Ryan, T., and Kim, H. J., 2013. "LMI-based gain synthesis for simple robust quadrotor control". *IEEE Transactions on Automation Science and Engineering*, **10**(4), pp. 1173–1178.
- [12] Raffo, G. V., Ortega, M. G., and Rubio, F. R., 2010. "An integral predictive/nonlinear H_∞ control structure for

- a quadrotor helicopter”. *Automatica*, **46**(1), pp. 29–39.
- [13] Mukherjee, P., and Waslander, S. L., 2012. “Direct adaptive feedback linearization for quadrotor control”. In Proceedings of the AIAA Guidance, Navigation, and Control Conference, pp. 2012–4917.
- [14] Zhong, Q.-C., and Rees, D., 2004. “Control of uncertain LTI systems based on an uncertainty and disturbance estimator”. *ASME Journal of Dynamic Systems, Measurement, and Control*, **126**(4), pp. 905–910.
- [15] Stobart, R. K., and Zhong, Q., 2011. “Uncertainty and disturbance estimator (UDE)-based control for uncertain LTI-SISO systems with state delays”. *Journal of Dynamic Systems, Measurement, and Control*, **133**(2), pp. 1–6.
- [16] Talole, S., and Phadke, S., 2008. “Model following sliding mode control based on uncertainty and disturbance estimator”. *Journal of Dynamic Systems, Measurement, and Control*, **130**, pp. 1–5.
- [17] Kuperman, A., and Zhong, Q.-C., 2010. “Robust control of uncertain nonlinear systems with state delays based on an uncertainty and disturbance estimator”. *International Journal of Robust and Nonlinear Control*, **21**(1), Mar., pp. 79–92.
- [18] Talole, S., and Phadke, S., 2009. “Robust input-output linearisation using uncertainty and disturbance estimation”. *International Journal of Control*, **82**(10), pp. 1794–1803.
- [19] Talole, S., Chandar, T. S., and Kolhe, J. P., 2011. “Design and experimental validation of UDE based controller-observer structure for robust input-output linearisation”. *International Journal of Control*, **84**(5), pp. 969–984.
- [20] Ren, B., Zhong, Q.-C., and Chen, J., 2015. “Robust control for a class of non-affine nonlinear systems based on the uncertainty and disturbance estimator”. *IEEE Transaction on Industrial Electronics*, **62**(9), pp. 5881–5888.
- [21] Kolhe, J. P., Shaheed, M., Chandar, T. S., and Taloe, S. E., 2013. “Robust control of robot manipulators based on uncertainty and disturbance estimation”. *International Journal of Robust and Nonlinear Control*, **23**, pp. 104–122.
- [22] Ren, B., and Zhong, Q.-C., 2013. “UDE-based robust control of variable-speed wind turbines”. In Proceedings of the 39th Annual Conference of the IEEE Industrial Electronics Society (IECON2013).
- [23] Phadke, S. B., and Taloe, S. E., 2012. “Sliding mode and inertial delay control based missile guidance”. *IEEE Transactions on Aerospace and Electronic Systems*, **48**(4), pp. 3331–3346.
- [24] Su, S., and Lin, Y., 2013. “Robust output tracking control for a velocity-sensorless vertical take-off and landing aircraft with input disturbances and unmatched uncertainties”. *International Journal of Robust and Nonlinear Control*, **23**, pp. 1198–1213.
- [25] Michael, N., Mellinger, D., Lindsey, Q., and Kumar, V., 2010. “The GRASP multiple micro-UAV testbed”. *IEEE Robotics & Automation Magazine*, **17**(3), pp. 56–65.